DSG3 as a biomarker for the ultrasensitive detection of occult lymph node metastasis in oral cancer using nanostructured immunoarrays

Vyomesh Patel [a], Daniel Martin [a], Ruchika Malhotra [b], Christina A. Marsh [a], Colleen L. Doçi [a], Timothy D. Veenstra [f], Cherie-Ann O. Nathan [c], Uttam K. Sinha [d], Bhuvanesh Singh [e], Alfredo A. Molinolo [a], James F. Rusling [b], J. Silvio Gutkind [a,*]

[a] Oral and Pharyngeal Cancer Branch, National Institute of Dental and Craniofacial Research, National Institutes of Health, Bethesda, MD 20892-4330, United States
[b] Departments of Chemistry and Cell Biology, University of Connecticut, Storrs, CT, United States
[c] Department of Otolaryngology, Head and Neck Surgery, Louisiana State University Health Sciences Center, Shreveport, LA, United States
[d] Department of Otolaryngology, Head and Neck Surgery, University of Southern California, Keck School of Medicine, Los Angeles, CA, United States
[e] Laboratory of Epithelial Cancer Biology, Head and Neck Service, Memorial Sloan-Kettering Cancer Center, New York, NY, United States
[f] Laboratory of Proteomics and Analytical Technologies, Science Applications International Corporation-Frederick, Inc., National Cancer Institute, Frederick, MD, United States

ARTICLE INFO

SUMMARY

Objectives: The diagnosis of cervical lymph node metastasis in head and neck squamous cell carcinoma (HNSCC) patients constitutes an essential requirement for clinical staging and treatment selection. However, clinical assessment by physical examination and different imaging modalities, as well as by histological examination of routine lymph node cryosections can miss micrometastases, while false positives may lead to unnecessary elective lymph node neck resections. Here, we explored the feasibility of developing a sensitive assay system for desmoglein 3 (DSG3) as a predictive biomarker for lymph node metastasis in HNSCC.
Materials and methods: DSG3 expression was determined in multiple general cancer- and HNSCC-tissue microarrays (TMAs), in negative and positive HNSCC metastatic cervical lymph nodes, and in a variety of HNSCC and control cell lines. A nanostructured immunoarray system was developed for the ultrasensitive detection of DSG3 in lymph node tissue lysates.
Results: We demonstrate that DSG3 is highly expressed in all HNSCC lesions and their metastatic cervical lymph nodes, but absent in non-invaded lymph nodes. We show that DSG3 can be rapidly detected with high sensitivity using a simple microfluidic immunoarray platform, even in human tissue sections including very few HNSCC invading cells, hence distinguishing between positive and negative lymph nodes.
Conclusion: We provide a proof of principle supporting that ultrasensitive nanostructured assay systems for DSG3 can be exploited to detect micrometastatic HNSCC lesions in lymph nodes, which can improve the diagnosis and guide in the selection of appropriate therapeutic intervention modalities for HNSCC patients.

Published by Elsevier Ltd.

Introduction

With more than 500,000 new cases annually, squamous cell carcinomas of the head and neck (HNSCC) represent one of the ten most common cancers globally,[1] and result in more than 11,000 deaths each year in the US alone.[2] The 5 year survival of newly diagnosed HNSCC patients is ∼50%, and despite new treatment approaches, it has improved only marginally over the past decades.[3] HNSCC has a high propensity to metastasize to loco-regional lymph nodes due to the presence of a rich lymphatic network and the overall high number of lymph nodes in the neck region.[3–8] Even in patients without clinical evidence of lymph node involvement (N0), there is a high incidence of occult lymph node metastasis, ranging from 10% to 50%.[4,5,7] The diagnosis of cervical lymph node metastasis an essential requirement for clinical staging and treatment,[9] and is now widely accepted as the most important factor in HNSCC prognosis.[3,5,6,10] However, due to limitations in the accurate diagnosis of lymph node metastasis, patients with clinically negative nodes often undergo elective neck resection or radiation,[11,12] with the consequent associated morbidity and adverse impact in the quality of life.[12]

Clinical assessments of lymph node metastases include physical examination, imaging modalities such as computed tomography (CT), magnetic resonance imaging (MRI), ultrasonography, and

* Corresponding author. Address: Oral and Pharyngeal Cancer Branch, National Institute of Dental and Craniofacial Research, NIH, 30 Convent Drive, Building 30, Room 211, Bethesda, MD 20892-4330, United States. Tel.: +1 301 496 6259; fax: +1 301 402 0823.
E-mail address: sg39v@nih.gov (J.S. Gutkind).

[^{18}F]-2-fluorodeoxyglucose positron emission tomography scans (PET).[13,14] However, poor spatial resolution, false positive detection of reactive lymph nodes, and limited sensitivity under 5 mm size,[15–18] can add to potential false negative results. Histopathological, immunohistochemical (IHC), and molecular approaches to evaluate sentinel lymph node biopsies have improved the detection rate of metastatic disease in some cancers,[19,20] but histopathology-based methods can often miss micrometastases, while more sensitive techniques such as IHC and real-time PCR for validated cancer markers are time consuming and require stringent handling procedures and technical expertise.

A recent proteomic analysis of paraffin embedded normal oral mucosa and HNSCC lesions revealed a very high abundance of Desmoglein 3 (DSG3) in both non-neoplastic epithelium and cancer lesions.[21] DSG3 is a transmembrane glycoprotein involved in cell-to-cell adhesion that is exclusively expressed in stratified epithelium.[22] These observations prompted us to explore whether the assessment of DSG3 protein levels could be used to investigate the presence of malignant squamous epithelial cells in cervical lymph nodes, and hence serve as a predictive biomarker for metastasis. In this regard, high sensitivity electrochemical immunoassays have recently gained acceptance in biomedicine.[23] For example, we have developed immunosensors based on nanostructured electrodes coupled to microfluidics and multilabel strategies to achieve highly sensitive detection of protein cancer biomarkers in serum.[24,25] We have combined these strategies into a simple microfluidic immunoarray[26,27] and here explore the suitability of this platform for the rapid and sensitive detection of DSG3 protein. We show that this system can be used to rapidly detect and quantify DSG3 in frozen human tissue sections, distinguishing between clinically positive and negative cervical lymph nodes. Overall, these studies may help develop point-of-care procedures aiding in the diagnosis of invaded lymph nodes in HNSCC patients, thereby facilitating educated decisions regarding appropriate therapeutic intervention modalities, and decreasing the morbidity often associated with HNSCC.

Materials and methods

Reagents, antibodies, and cell culture

All chemicals and reagents were from Sigma–Aldrich (St. Louis, MO), unless indicated. The following antibodies: goat-anti-human DSG3 [AF1720]; mouse-anti-human DSG3 [MAP1720], biotin labeled goat-anti-human DSG3 [BAF1720], recombinant human DSG3 Fc Chimera protein [1720-DM], were from R&D Systems (MN, USA). The mouse anti-human DSG3 antibody [32-6300] from Invitrogen (MA, USA), and rabbit-anti-cytokeratin Wide Spectrum Screening [N1512] from Dako (CA), were used for immunohistochemistry (IHC). The α-tubulin antibody [11H10] was from Cell Signaling Technology (MA, USA). Biotinylated peroxidase and streptavidin coated magnetic beads were from Invitrogen. Anti-rabbit and anti-mouse biotinylated secondary antibodies were from Vector, Burlingame, CA, US. HN12, HN13 and HN30 cells were described previously.[28] Cal27 and Jurkat cells were from ATCC (VA); and primary human cells from Lonza (MD). See Supplemental information for additional information.

Human clinical tissues and tissue microarrays (TMAs), immunohistochemistry and immunofluorescence

Formalin fixed, paraffin-embedded, and freshly frozen HNSCC and lymph node samples were obtained anonymized with Institutional Review Board approval. Five μm sections from all tissues underwent standard H&E staining for histopathological evaluation and immunostaining. Tissue microarrays used include TMA MC2081 US (Biomax, MD) with 208 representative cases of colorectal, breast, prostate and lung cancers, and normal tissue; TMA LC810 (Biomax, MD), consisting of 40 cases of different types of lung cancers with their matched metastatic lymph nodes (total 80 tissue cores); and the Head and Neck Tissue Microarray Initiative, including 317 HNSCC cases.[29] Tissue processing and analysis are described in detail in Supplemental information. All slides were scanned at 400× magnification using an Aperio CS Scanscope (Aperio, CA) and quantified using the available Aperio algorithms. Immunodetection of DSG3 was quantified according to percent of tumor cells stained (1–25%, 26–50%, 51–75%, or 76–100%).[29] For immunofluorescence, 10 μm cryosections were immunostained with goat-anti-human DSG3 (AF1720), mouse-anti-vimentin and DAPI containing. See Supplemental information for additional details.

Western blot analysis of cell and tissue extract, and microfluidic immunoarrays systems for DSG3

A detailed description of the procedures used for tissue lysate preparation, SDS–PAGE gel analysis and Western blotting, and the fabrication of the microfluidic immunoarrays made of gold nanoparticles layered with glutathione are described in detail in the Supplemental information. Briefly, the immunoarrays consisting of eight sensor elements, made of gold nanoparticles layered with glutathione, were first coated with the capture antibody and transferred to a microfluidic chamber. In parallel, biotinylated horseradish peroxidase and a biotinylated secondary antibody were attached to streptavidin-coupled magnetic beads and collected with a magnet. Next, 5 μl of 5–750 fg/mL of recombinant DSG3 protein standards or 4 μl tissue extract were diluted 1:6000 in RIPA buffer and added to the bioconjugates. The bioconjugates with captured proteins were then magnetically separated, washed, resuspended in a final volume of 110 μL, and immediately injected into the microfluidic channel housing the immunoarrays. At this step, the flow was stopped, incubated for 20 min, washed, and hydroquinone solution was passed through the channel. The amperometric signal was developed by injecting 50 μL of 100 μM H_2O_2. Tissue lysates used for Western blot analysis and microfluidic immunoarrays were made from primary tumors ($n = 4$), lymph node (−) ($n = 3$), and lymph node (+) ($n = 3$).

Results

In a previous proteome-wide analysis of HNSCC progression, we noted that DSG3 was highly expressed in normal oral mucosa and HNSCC lesions.[21] To further investigate a possible use for DSG3 as a predictive biomarker, we first assessed DSG3 expression by immunohistochemistry in an independent cohort of human normal and malignant oral squamous tissues. By H&E histological evaluation, normal squamous epithelium shows a defined basement membrane with layers of differentiating keratinocytes, whereas in the malignant counterpart, this organized pattern is lost (Fig. 1A). Normal tissues sections stained for DSG3 show that it is predominantly expressed in the basal and suprabasal layers of the normal squamous epithelium, while in SCC DSG3 expression is restricted to cancer cells. Stromal cells were negative. We next evaluated DSG3 expression in a HNSCC tissue microarray (TMA) containing 317 evaluable cores.[29] DSG3 was readily detected in all HNSCC cores and localized to tumors cells (Fig. 1B). Within these cases, well-differentiated carcinomas ($n = 120$) had the highest percentage of DSG3-positive cells (∼90%). The moderate- ($n = 119$), and poorly-differentiated ($n = 66$) cores showed slightly lower proportion of DSG-reactive cells (80% and 70%, respectively), the remaining 12 cores consisting of corresponding to non-squamous tissues were
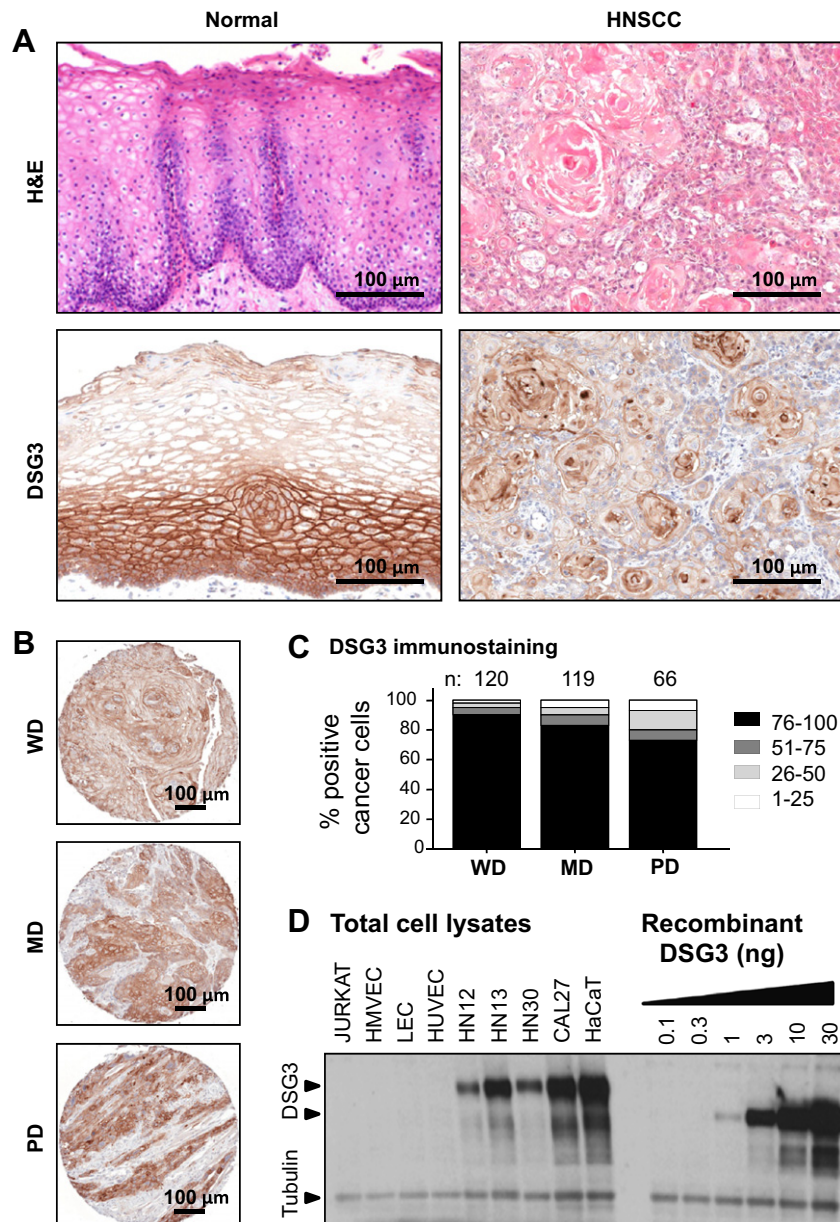
Figure 1 Validation of DSG3 expression in normal and malignant HNSCC. Normal oral mucosa biopsies and HNSCC were evaluated for DSG3 by IHC. (A) DSG3 is expressed throughout the normal epithelium, but is stronger in the basal and parabasal layers. Diffuse expression was seen in the epithelial component of all HNSCC. (B) Representative well (WD), moderate (MD) and poorly (PD) differentiated HSCC cases are shown. (C) DSG3 was expressed in all tumors regardless of differentiation, with increased expression in WD cases. Numbers of cases analyzed is depicted. (D) Total cell extracts from non-squamous (Jurkat, HMVEC, LEC, HUVEC) and oral-squamous (HN12, HN13, HN30, Cal27), and epidermal-squamous (HaCaT) were processed for Western blot analysis. Native DSG3 and its glycosylated forms were readily detected in squamous cells extracts, while absent from the non-squamous counterparts. These levels were compared with human recombinant DSG3 that was processed in a background of Jurkat cell lysate. Tubulin staining indicates equivalent loading and protein integrity.

negative for DSG3 (Fig. 1C). The data demonstrates that DSG3 is highly expressed in human oral squamous epithelium and HNSCC.

We next sought to assess *in vitro* the specificity of the epithelial expression of DSG3 in a panel of squamous and non-squamous model cells. The latter included Jurkat cells (immortalized T lymphocyte cells), HMVEC (skin human microvascular endothelial cells), LEC (lymphatic endothelial cells), and HUVEC (human umbilical vein endothelial cells). HaCaT cells are squamous, non-oral immortalized epidermal keratinocytes, while the oral squamous cell carcinoma lines included HN12, HN13, HN30 and Cal27.[28] DSG3 was readily detected in all squamous oral cancer cell lines and HaCaT cells, with lower levels in HN12 and higher in Cal27 (Fig. 1D). No expression for DSG3 was observed in any of four non-squamous lines, while levels of α-tubulin indicated equal loading as well as protein integrity. The data seem to indicate that DSG3 is exclusively expressed in squamous epithelial-derived cells.

To further validate the specificity of DSG3 expression, we evaluated TMAs containing cores representing the four most common cancers (breast, lung, prostate, and colon cancer) for DSG3 levels, and scored cases based on the presence or absence of DSG3 expression. As seen in Fig. 2A), DSG3 is poorly expressed in breast and prostate cancers, as well in adenocarcinoma of the lung (ADC), which likely reflects the glandular epithelial cell origin of these human malignancies. In colon carcinoma, the expression was variable, and in all cases the pattern of expression was diffused and not the characteristic membrane lace-like pattern. In contrast,
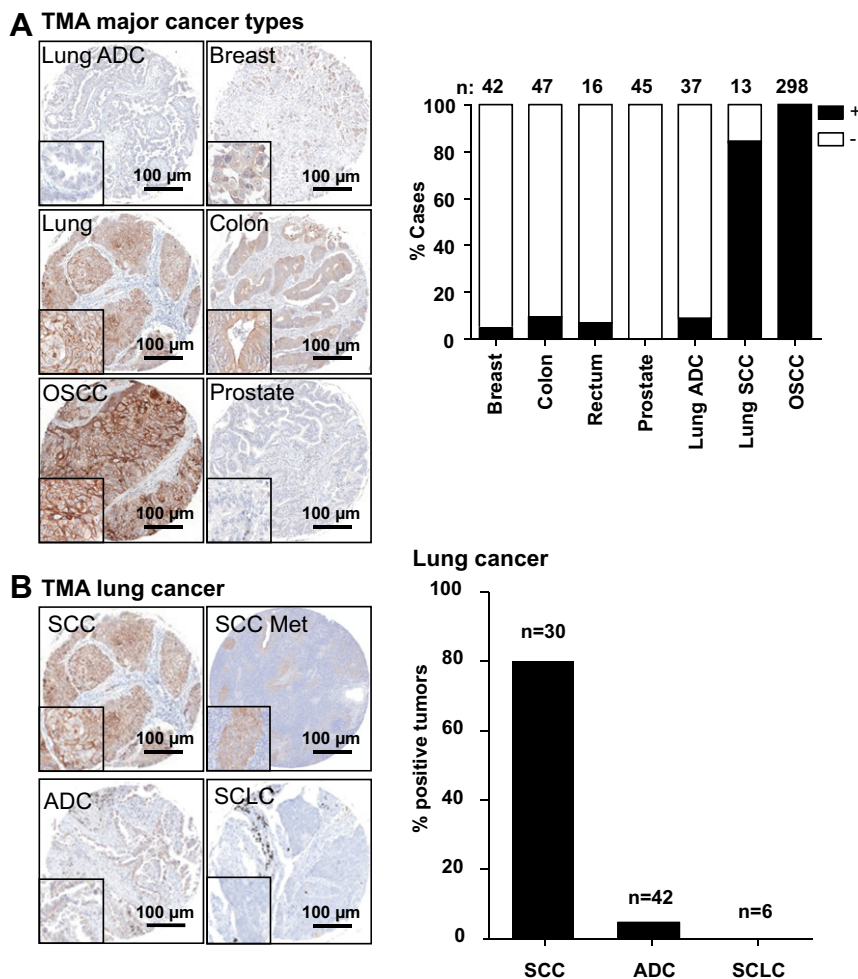
A TMA major cancer types

B TMA lung cancer

Figure 2 Immunoreactivity of DSG3 in common tumor types. (A) Multi-tumor TMAs (lung, breast, colon, prostate), and an oral specific TMA were assessed for DSG3 expression by IHC, and the staining scored for the presence of specific staining as (+) or (−). Most squamous cell lung cancers stained positive for DSG3, but very few of the adenocarcinomas gave positive reaction. All cores from the OSCC TMA scored positive. (B) In lung cancer, DSG3 expression was positive in most squamous cell carcinomas (SCC) including lymph node metastasis (SCC Met), while few cases of adenocarcinomas (ADC) gave positive reaction, and all small cell lung carcinoma samples (SCLC), were negative.

DSG3 is highly expressed in tumors derived from cells of squamous epithelial origin, such as lung squamous carcinoma (SCC) and additional oral squamous carcinoma (OSCC) that were included in these arrays, showing a membrane localized staining. All stainings were scored blindly and tabulated (Fig. 2A). All cancers of squamous origin (oral and lung SCC) were strongly positive for DSG3 expression. As lung cancers include SCC, ADC, and small cell lung carcinomas (SCLCs), we examined further the specificity of DSG3 expression in these distinct lung cancer lesions. All lung SCC show strong membrane localized staining in both the primary tumor and metastasis, while ADC and SCLC show marginal to no DSG3 expression, as reflected by scoring their corresponding tissue cores (Fig. 2B). Collectively, our results indicate the high specificity of DSG3 expression in oral and lung SCC lesions.

Based on the observation that DSG3 is highly expressed in HNSCC, we wanted to determine if the presence of this protein in cervical lymph nodes of the neck region could be used as a predictive biomarker of HNSCC invasion. To this end, we evaluated formalin-fixed, paraffin-embedded and anonymized tissue sections of non-metastatic (N0) or metastatic (N+) human cervical lymph node biopsies from patients diagnosed with HNSCC for expression of DSG3 and cytokeratin, a squamous-specific protein marker. Negative lymph nodes were negative (Fig. 3A) whereas clusters of tumor cells stained positive for membrane-localized DSG3

(inset, top right), can be seen throughout the invaded lymph node (N+), indicating the metastatic spread of squamous tumor cells of the primary tumor lesions from the oral cavity (Fig. 3A). Noteworthy, small clusters of 2–3 isolated tumor cells, constituting micrometastases were readily detected by the presence of DSG3 protein, and this size tumor island could potentially be missed by histopathological evaluation (Inset). Next, we screened a larger cohort of metastatic and non-metastatic human cervical lymph nodes for cytokeratin and DSG3 expression ($n = 35$). All metastatic ($n = 30$), but not non-metastatic cases ($n = 5$) were positive for DSG3. Serial sections stained for H&E and cytokeratin confirmed the epithelial nature of the malignant DSG3-positive cells. (Fig. 3B, and low magnification of a whole lymph node in Suppl. Fig. 1). This indicates that DSG3 expression can help identify small numbers of malignant squamous tumor cells in lymph nodes, and hence the metastatic nature of the primary lesion. The sensitivity and specificity of this detection suggests that DSG3 may hold promise for accurately detecting micrometastasis in cervical lymph nodes in newly diagnosed HNSCC patients.

Our previous study adapted amperometric sandwich immunoassays to a microfluidic system for the ultrasensitive, multiplexed detection of secreted biomarker proteins.[26] Here, we used a similar strategy for detecting DSG3 in complex tissue extracts using the microfluidic immunoassay system. As shown in Fig. 4A, DSG3
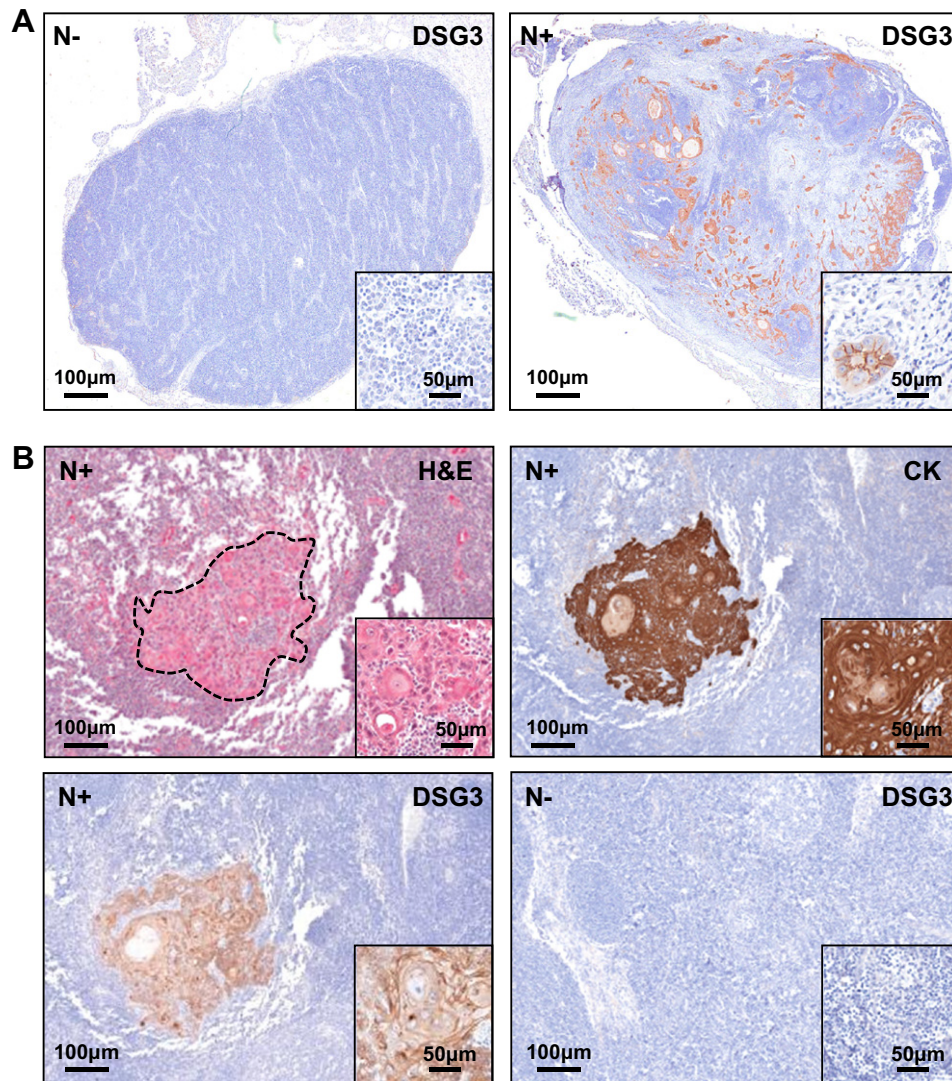
Figure 3 Specific detection of DSG3 in human cervical lymph nodes. (A) Formalin fixed and paraffin embedded tissue sections of non-metastatic (N−) and metastatic lymph nodes (N+) show DGS3 expression only in N+, with the staining localized to the malignant squamous cells (n = 30). All N− cases were negative (n = 5). B. The epithelial specificity of DSG3 immunoreactivity was further confirmed using simultaneous cytokeratin (CK) staining. A representative example is shown, whereby the H&E stained tumor island is matched with CK and DSG3 expression, with no non-specific staining. An example of a N− case stained for DSG3 is shown.

capture antibodies are attached to up 8 sensor elements, and strep-tavidin-coated paramagnetic beads (MB) loaded with 400,000 biotin-HRPs and thousands of secondary biotin-labeled antibodies to DSG3 (Ab$_2$) are used to capture the protein off-line. After washing and magnetic separation, the MBs that have bound DSG3 (DSG3-MB) are injected into the microfluidic channel. Incubation at stopped flow allows the sensor antibodies to capture DSG3-MBs, and amperometric signals are developed by injecting hydrogen peroxide to activate HRP and hydroquinone to mediate the amperometic oxidation, resulting in peak currents proportional to DSG3 concentration (Fig. 4B). Noteworthy, the entire assay from incubation of sample with Ab$_2$-MB-HRP to measurement takes ∼50 min. Remarkably, using this approach we were able to accurately and reproducibly detect DSG3 protein at levels down to 5 fg mL^{-1} in complex tissue extracts, with minimal non-specific binding.

We next used these protocols for capturing DSG3 from clinical samples of human HNSCC. Desmosomes are notoriously insoluble, and multiple buffers tested, RIPA buffer afforded excellent solubility and retaining antigenicity of DSG3 extracted directly from cryosections of HNSCC and lymph node tissue. Protein extracts were made from a single 10 μm cryosection from each sample and used as

input. Picogram levels of DSG3 protein were detected in all tumor samples (T1–4), and this was confirmed by Western blot analysis, where high levels of the protein were also detected in total cell extracts that were used for these analyses (Fig. 4C and D).

The specificity of DSG3 identification was further confirmed by simultaneous fluorescence microscopy of DSG3 and vimentin, as a stromal marker, in frozen sections of a series of metastatic and non-metastatic lymph nodes. As seen in Fig. 5A, only vimentin (red) was identified in non-metastatic lymph nodes (in blue, nuclear DAPI staining), whereas all metastatic lymph nodes showed pockets of very strong staining for DSG3 (green).

To further explore the sensitivity of the method, we decided to analyze metastatic lymph node tissues in which the number of malignant epithelial cells was known. For this, H&E stained slides of each case was scanned, analyzed histologically, the malignant areas identified, and the number of cells quantified using the Aperio nuclear algorithm (Aperio, Vista, CA). The number of cancer cells per lymph node section is indicated in Table 1. No tumor cells were be present in the negative lymph nodes, while all three metastatic lymph nodes (1–3) evaluated had differing number of tumor cells. Noteworthy, positive lymph node 1 had less than
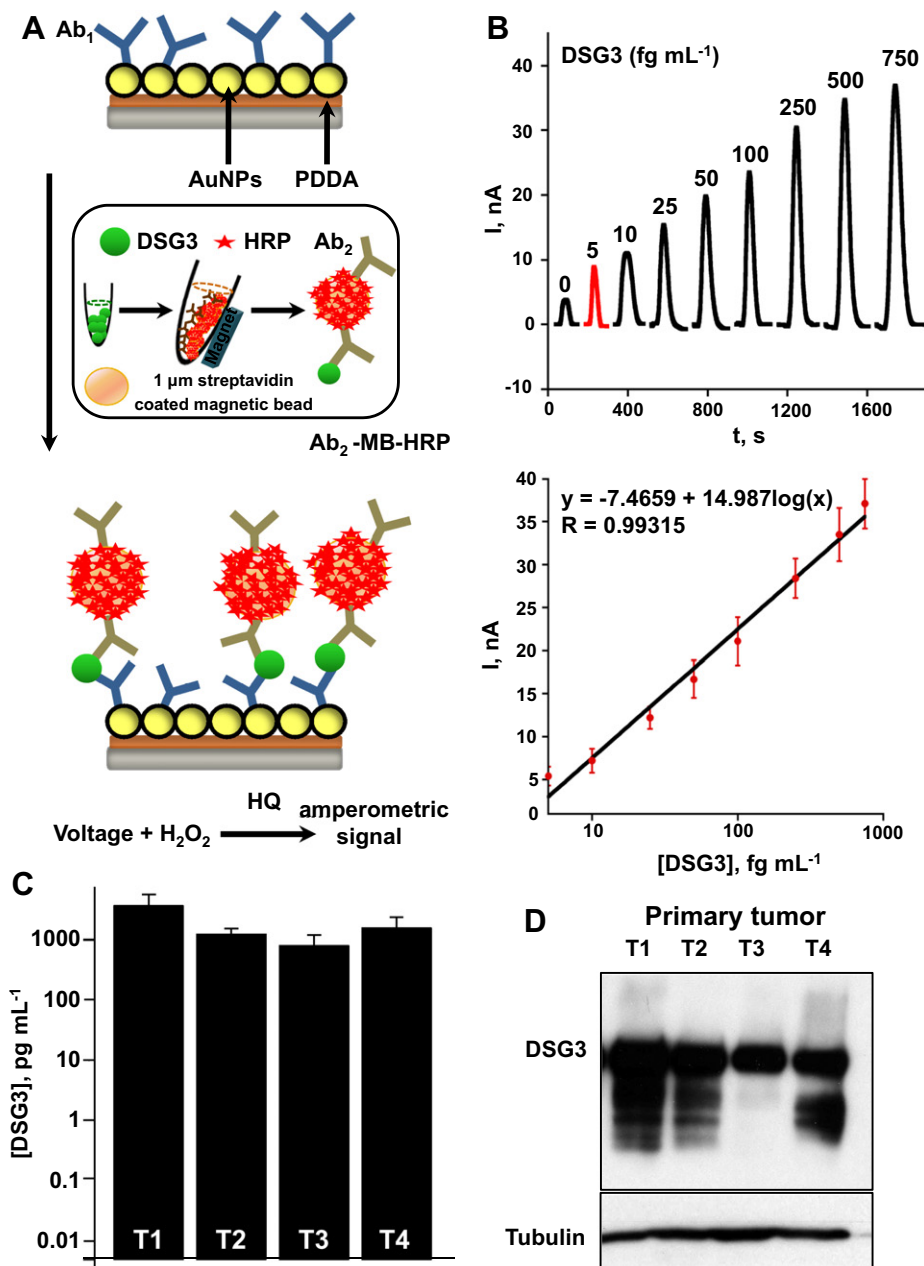
Figure 4 Rapid and ultrasensitive detection of DSG3 in human HNSCC samples using nanosensors. (A) Scheme used for the ultrasensitive detection by the microfluidic immunoarray showing a single sensor in the array with capture DSG3 antibodies attached. Proteins are captured off-line on Ab2-magnetic bead (MB)-HRP bioconjugates , and after magnetic separation and washes, the MBs are injected into the immunoarray containing 8 sensors. A single immunoarray sensor is depicted. Following incubation, amperometric signals are generated by applying −0.3 V versus Ag/AgCl to the sensors by injecting a mixture of HRP-activator H_2O_2 and mediator hydroquinone (HQ). (B) Varying recombinant DSG3 protein concentrations were used to generate a calibration plot. The sensitivity of DSG3 sensor using recombinant protein was 5646 nA mL [fg protein]$^{-1}$ cm^{-2}. (C) Protein extracts of primary human oral squamous carcinomas (T1–4) made with RIPA buffer were processed for detection of DSG3. High DSG3 levels were found to be present in all the samples, and this was confirmed by Western blot analysis of the same extracts for DSG3 (D). Tubulin was used as loading control.

1000 tumor cells, while the remaining had between 13,000 and 16,000 cells (Table 1). Using the nanosensors, we evaluated total protein extracts from lymph nodes for levels of DSG3. As seen in Fig. 5A, DSG3 was essentially not detected in the normal lymph nodes, with marginal values likely a reflection of very limited residual non-specific binding of Ab2-MB-HRP complex, giving rise to minimal amperometric signal. In contrast, all of the positive, metastatic lymph nodes showed high levels of DSG3 protein expression. To validate these measurements, the same protein extracts were also analyzed by Western blotting (Fig. 5B). No DSG3 was detected in the negative lymph nodes, while in all the positive lymph nodes, bands for DSG3 and its multiple glycosylated forms were readily seen, and

the intensity of the corresponding bands correlated with DSG3 levels quantified by the nanosensors. When total DSG3 was normalized by the number of tumor cells in each metastatic lesion, positive lymph nodes expressed approximately 150 fg DSG3 per tumor cell (Table 1), well above the threshold for DSG3 detection. Together, this indicates that the nanosensor-based detection of DSG3 could be a highly sensitive and specific method for the identification of squamous carcinoma metastases in clinical practice. This rapid method was capable of measuring DSG3 levels even from as little as a single cell, suggesting that this technique may represent a potent tool for the ultrasensitive detection of the presence or absence of lymph node invasion in human oral cancer patients.
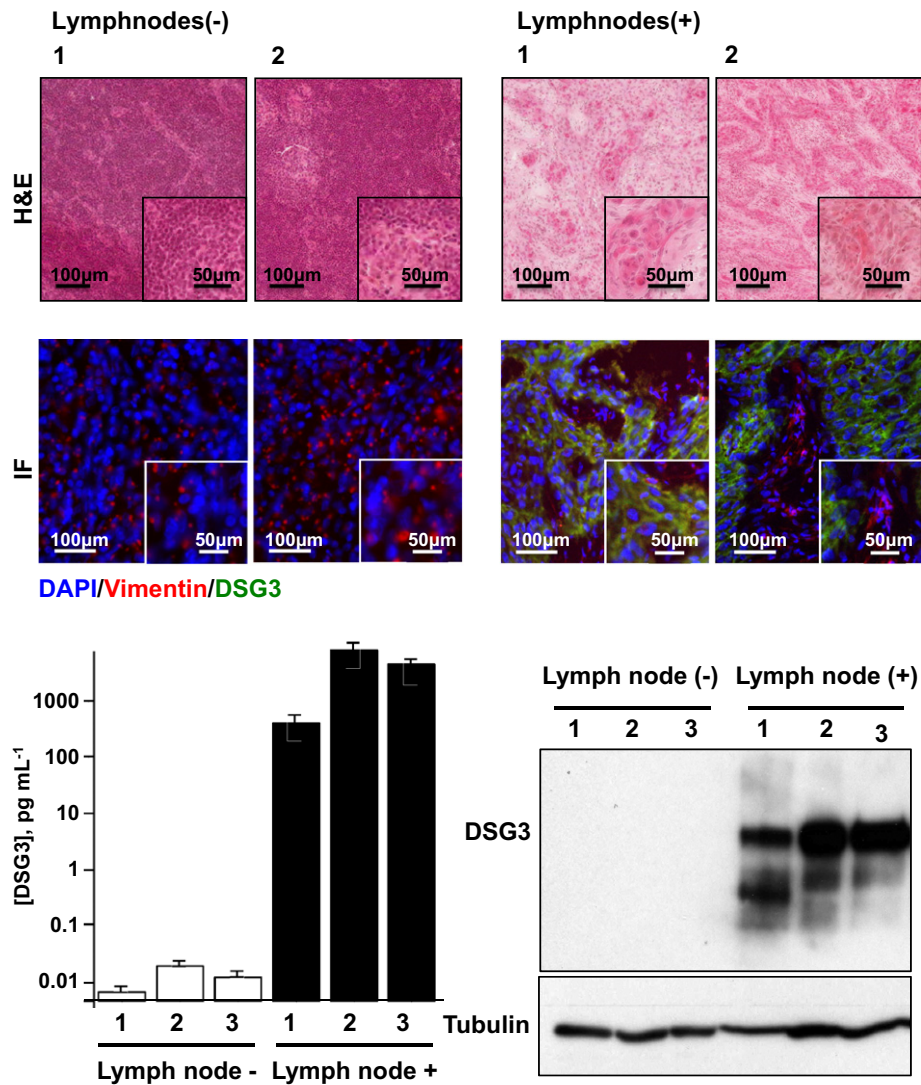
Figure 5 Detection of DSG3 in metastatic human cervical lymph nodes. H&E stained cryosections of representative non-metastatic (−) and metastatic (+) human cervical lymph nodes were scanned and the total number of tumor cells per section was quantified (Table 1). Serial sections of these lymph nodes were evaluated by immunofluorescence for DSG3 and detected only in metastatic lymph nodes (green). Vimentin (red) was used to identify stromal tissue, and nuclei of all cells were stained blue with DAPI (Fig. 5A). Protein extracts made from single cryosections of lymph nodes were used for the detection of DSG3 by Western blot analysis and DSG3 quantification using nanosensors. DSG3 levels were similar to background for all non-metastatic samples, while DSG3 levels in all metastatic cases were proportional to the number of invading HNSCC cells (Fig. 5B).

Table 1
DSG3 detection in metastatic lymph nodes. Cryosections of non-metastatic (N−) (n = 3) and metastatic (N+) (n = 3) human cervical lymph nodes were collected and analyzed by nanosensor detection. The total number of tumor cells per cryosection was evaluated, and used to estimate the total amount of DSG3 per tumor cell.

Samples	Detected DSG3 (pg/mL)	Tumor cells per section	Detected DSG3 (fg/tumor cell)
N−1	0.01	–	–
N−2	0.03	–	–
N−3	0.02	–	–
N+1	427	697	202
N+2	6274	13,843	150
N+3	4512	16,576	90

Discussion

The spread of primary HNSCC lesions to locoregional lymph nodes has often already occurred at the time of diagnosis, thus compromising the prognosis and long-term survival of HNSCC patients.[3] Accurate diagnosis of lymph node metastases remains difficult, and many patients that do not present cancer dissemination to the lymph nodes (N0) may be subjected to unnecessary elective surgery.

On the other hand, small lesions may be difficult to identify within the lymph nodes in cryosections when histophatologic evaluation is performed while the patient is in the operating room. Hence, some patients may miss a therapeutic opportunity due to false negative diagnosis of lymph node metastasis. Here, we demonstrate that DSG3 is expressed in normal oral squamous mucosa, and in all HNSCC lesions and their metastatic cervical lymph nodes. Indeed, the presence of DSG3 in lymph nodes can be exploited to detect

micrometastatic lesions, which can serve as a sensitive marker of HNSCC progression. We also show the feasibility of using a rapid, low-cost nanostructured immunoarray device for the detection of DSG3 protein in metastatic lymph nodes in newly diagnosed HNSCC patients, which can improve diagnosis and guide the most effective therapeutic options.

Most current technologies for cancer detection and diagnostics are not suitable for the differentiation of normal versus metastatic lymph nodes at early stages of cancer progression, and efforts to address this gap have been met with mixed results. Currently, the gold standard for identification of metastasis is the serial sectioning and histopathological analysis of tissue specimens by H&E staining and immunohistochemistry.[30] This provides key information needed for TNM (tumor-node-metastasis criteria) classification of HNSCC patients. However, a risk remains that micrometastases may go undetected in otherwise negative lymph nodes. IHC performed on serial sections for cytokeratin may help in detecting metastases, but unfortunately this low-throughput method requires significant investment of time and expense, and it is often performed after surgery. Considering the false-negative rate and the sampling error that are encountered by H&E examination alone, a reliable and rapid predictive test to determine lymph node metastases is needed.[31]

Application of new technologies such as real-time quantitative PCR (qPCR), to look at mRNA levels of molecules expressed by oral squamous tissues have shown encouraging results.[32] While this improves upon some of the limitations of IHC detection of cytokeratins, independent studies have found some inconsistencies in the precise cytokeratin to be analyzed. For example, from a three-marker analysis, only cytokeratin 14 was reliably detected by qPCR in several oral cancer cell lines and tissues, and sensitive enough to detect down to a single cancer cell in a background of Jurkat cells, essentially representing a model of lymph node metastasis.[33] In another study, cytokeratin 17 was demonstrated to be far superior at discriminating positive lymph nodes while cytokeratin 14 was less informative, although in parallel histological analysis, this was only achieved if metastasis had exceeded 450 µm, leaving a high probability of micrometastasis going undetected.[34] While the sensitivity of qPCR for detecting cytokeratins is unquestionable, its ability to reliably and consistently detect these molecules in a single tumor cell embedded within normal lymphatic tissues still remains a challenge.

The met-receptor is over-expressed in several metastatic carcinomas including HNSCC,[35,36] and with minimal to none in lymphatic cells, its presence in lymph nodes may be exploited for predicting metastasis. Indeed, qPCR analysis detected met expression in 40% of invaded lymph nodes, and interestingly exceeding the sensitivity of cytokeratins, which were tested in the same sample cohort.[37] Use of multiple markers may improve detection of metastatic lymph nodes, and in this regard, mRNA for DSG3 (referred to as pemphigus vulgaris antigen, PVA) and TACSTD1 (tumor-associated calcium signal transducer 1), have been previously reported to be highly expressed in HNSCC, and successfully integrated into a multiplex qRT-PCR assay for metastatic prediction, achieving a remarkable accuracy.[38,39] DSG3 mRNA levels in lymph nodes have been also touted as potential predictors of HNSCC progression.[38,40] Generally, the use of qPCR greatly improves the sensitivity of detection of target genes, but the need of high quality RNA extracted from tissues remains a significant technical hurdle, such as the presence of contaminants and RNA degradation that can severely interfere with data interpretation. It is noteworthy that mRNA levels may not accurately reflect protein expression, as many post translational regulatory processes may allow or prevent the accumulation of translated products, and for predictive biomarkers, the presence of the target protein may be better suited.

In this regard, our proteomics analysis of HNSCC and normal oral epithelial tissues suggested that DSG3 is preferentially expressed in squamous tissues.[21] By examining hundreds of cancer lesions representing some of the most prevalent human malignancies we now show that DSG3 is highly expressed in all tumors derived from cells of squamous epithelial origin, such as lung SCC and HNSCC, with more variable expression in adenocarcinomas of the colon, prostate, breast and lung, likely reflecting their glandular epithelial cell of origin. For HNSCC, we noticed a lower expression of DSG3 in poorly differentiated lesions, aligned with prior reports.[41] However, all HNSCC cases analyzed expressed DSG3, albeit in some lesions not all tumor cells expressed this marker. Thus, although the possibility exists that in some invaded lymph nodes the level of DSG3 may be below our detection limit, our collective findings indicate that DSG3 is highly expressed in all human SCCs but not expressed in normal lymph nodes, and that DSG3 can be detected even in small clusters of malignant cells invading the lymph nodes, thus serving as a marker for the metastatic spread of the cancerous lesions. We now exploited this information, the availability of highly specific monoclonal antibodies detecting different epitopes in DSG3, and our recently established biomarker detection platform using microfluidic immunoarray devices featuring nanostructured electrodes,[26] to develop an assay system enabling the rapid and ultrasensitive detection of DSG3 protein in complex tissue extracts, with minimal non-specific binding. The method was sensitive enough to detect isolated tumor cells, and certainly small groups of cells in a single cryosection of a positive lymph node.

Taken together, we can conclude that the ability to quantitate femtogram levels of DSG3 can be used for the intraoperational detection of the presence of even few invasive human squamous epithelial cells in cryosections of lymph nodes of HNSCC patients, hence aiding the pathologists and surgeons to make informed decisions about appropriate treatment options. We expect that similar approaches can be used to optimize the detection of additional cancer biomarkers in lymph node sections, thus increasing the basis for successful clinical prediction. Collectively, combined with a simple work-flow and a short assay time, these features described in this study, hold promise for the development of point-of-care clinical screening techniques to identify HNSCC patients with metastatic disease. Indeed, the encouraging results described in this proof of principle study may provide the rationale for future validation of this diagnostic strategy in larger multicenter studies.

Conflict of interest statement

None declared.

Acknowledgements

Appendix A. Supplementary material

Supplementary data associated with this article can be found, in the online version, at http://dx.doi.org/10.1016/j.oraloncology.2012.08.001.

References

1. Ferlay J, Shin HR, Bray F, Forman D, Mathers C, Parkin DM. Estimates of worldwide burden of cancer in 2008: GLOBOCAN 2008. *Int J Cancer* 2010;**127**(12):2893–917.
2. Siegel R, Naishadham D, Jemal A. Cancer statistics, 2012. *CA Cancer J Clin* 2012;**62**(1):10–29.

3. Forastiere A, Koch W, Trotti A, Sidransky D. Head and neck cancer. *N Engl J Med* 2001;**345**(26):1890–900.

4. Clark JR, Naranjo N, Franklin JH, de Almeida J, Gullane PJ. Established prognostic variables in N0 oral carcinoma. *Otolaryngol Head Neck Surg* 2006;**135**(5):748–53.

5. Kuriakose MA, Trivedi NP. Sentinel node biopsy in head and neck squamous cell carcinoma. *Curr Opin Otolaryngol Head Neck Surg* 2009;**17**(2):100–10.

6. Leemans CR, Tiwari R, Nauta JJ, van der Waal I, Snow GB. Recurrence at the primary site in head and neck cancer and the significance of neck lymph node metastases as a prognostic factor. *Cancer* 1994;**73**(1):187–90.

7. Shah JP, Candela FC, Poddar AK. The patterns of cervical lymph node metastases from squamous carcinoma of the oral cavity. *Cancer* 1990;**66**(1):109–13.

8. Vokes EE, Weichselbaum RR, Lippman SM, Hong WK. Head and neck cancer. *N Engl J Med* 1993;**328**(3):184–94.

9. Snow GB, Annyas AA, van Slooten EA, Bartelink H, Hart AA. Prognostic factors of neck node metastasis. *Clin Otolaryngol Allied Sci* 1982;**7**(3):185–92.

10. Mamelle G, Pampurik J, Luboinski B, Lancar R, Lusinchi A, Bosq J. Lymph node prognostic factors in head and neck squamous cell carcinomas. *Am J Surg* 1994;**168**(5):494–8.

11. Weiss MH, Harrison LB, Isaacs RS. Use of decision analysis in planning a management strategy for the stage N0 neck. *Arch Otolaryngol Head Neck Surg* 1994;**120**(7):699–702.

12. Bar Ad V, Chalian A. Management of clinically negative neck for the patients with head and neck squamous cell carcinomas in the modern era. *Oral Oncol* 2008;**44**(9):817–22.

13. Cianchetti M, Mancuso AA, Amdur RJ, Werning JW, Kirwan J, Morris CG, et al. Diagnostic evaluation of squamous cell carcinoma metastatic to cervical lymph nodes from an unknown head and neck primary site. *Laryngoscope* 2009;**119**(12):2348–54.

14. van den Brekel MW, Castelijns JA, Stel HV, Golding RP, Meyer CJ, Snow GB. Modern imaging techniques and ultrasound-guided aspiration cytology for the assessment of neck node metastases: a prospective comparative study. *Eur Arch Otorhinolaryngol* 1993;**250**(1):11–7.

15. Troost EG, Vogel WV, Merkx MA, Slootweg PJ, Marres HA, Peeters WJ, et al. 18F-FLT PET does not discriminate between reactive and metastatic lymph nodes in primary head and neck cancer patients. *J Nucl Med* 2007;**48**(5):726–35.

16. Ozer E, Naiboglu B, Meacham R, Ryoo C, Agrawal A, Schuller DE. The value of PET/CT to assess clinically negative necks. *Eur Arch Otorhinolaryngol* 2012.

17. Yamazaki Y, Saitoh M, Notani K, Tei K, Totsuka Y, Takinami S, et al. Assessment of cervical lymph node metastases using FDG-PET in patients with head and neck cancer. *Ann Nucl Med* 2008;**22**(3):177–84.

18. Schoder H, Carlson DL, Kraus DH, Stambuk HE, Gonen M, Erdi YE, et al. 18F-FDG PET/CT for detecting nodal metastases in patients with oral cancer staged N0 by clinical examination and CT/MRI. *J Nucl Med* 2006;**47**(5):755–62.

19. Phan GQ, Messina JL, Sondak VK, Zager JS. Sentinel lymph node biopsy for melanoma: indications and rationale. *Cancer Control* 2009;**16**(3):234–9.

20. Salhab M, Patani N, Mokbel K. Sentinel lymph node micrometastasis in human breast cancer: an update. *Surg Oncol* 2011;**20**(4):e195–206.

21. Patel V, Hood BL, Molinolo AA, Lee NH, Conrads TP, Braisted JC, et al. Proteomic analysis of laser-captured paraffin-embedded tissues: a molecular portrait of head and neck cancer progression. *Clin Cancer Res* 2008;**14**(4):1002–14.

22. Amagai M, Stanley JR. Desmoglein as a target in skin disease and beyond. *J Invest Dermatol* 2012;**132**(3 Pt 2):776–84.

23. Rusling JF, Kumar CV, Gutkind JS, Patel V. Measurement of biomarker proteins for point-of-care early detection and monitoring of cancer. *Analyst* 2010;**135**(10):2496–511.

24. Munge BS, Coffey AL, Doucette JM, Somba BK, Malhotra R, Patel V, et al. Nanostructured immunosensor for attomolar detection of cancer biomarker interleukin-8 using massively labeled superparamagnetic particles. *Angew Chem Int Ed Engl* 2011;**50**(34):7915–8.

25. Malhotra R, Patel V, Vaque JP, Gutkind JS, Rusling JF. Ultrasensitive electrochemical immunosensor for oral cancer biomarker IL-6 using carbon nanotube forest electrodes and multilabel amplification. *Anal Chem* 2010;**82**(8):3118–23.

26. Chikkaveeraiah BV, Mani V, Patel V, Gutkind JS, Rusling JF. Microfluidic electrochemical immunoarray for ultrasensitive detection of two cancer biomarker proteins in serum. *Biosens Bioelectron* 2011;**26**(11):4477–83.

27. Chikkaveeraiah BV, Bhirde A, Malhotra R, Patel V, Gutkind JS, Rusling JF. Single-wall carbon nanotube forest arrays for immunoelectrochemical measurement of four protein biomarkers for prostate cancer. *Anal Chem* 2009;**81**(21):9129–34.

28. Jeon GA, Lee JS, Patel V, Gutkind JS, Thorgeirsson SS, Kim EC, et al. Global gene expression profiles of human head and neck squamous carcinoma cell lines. *Int J Cancer* 2004;**112**(2):249–58.

29. Molinolo AA, Hewitt SM, Amornphimoltham P, Keelawat S, Rangdaeng S, Meneses Garcia A, et al. Dissecting the Akt/mammalian target of rapamycin signaling network: emerging results from the head and neck cancer tissue array initiative. *Clin Cancer Res* 2007;**13**(17):4964–73.

30. Broglie MA, Haile SR, Stoeckli SJ. Long-term experience in sentinel node biopsy for early oral and oropharyngeal squamous cell carcinoma. *Ann Surg Oncol* 2011;**18**(10):2732–8.

31. Leong SP, Zuber M, Ferris RL, Kitagawa Y, Cabanas R, Levenback C, et al. Impact of nodal status and tumor burden in sentinel lymph nodes on the clinical outcomes of cancer patients. *J Surg Oncol* 2011;**103**(6):518–30.

32. Elsheikh MN, Rinaldo A, Hamakawa H, Mahfouz ME, Rodrigo JP, Brennan J, et al. Importance of molecular analysis in detecting cervical lymph node metastasis in head and neck squamous cell carcinoma. *Head Neck* 2006;**28**(9):842–9.

33. Becker MT, Shores CG, Yu KK, Yarbrough WG. Molecular assay to detect metastatic head and neck squamous cell carcinoma. *Arch Otolaryngol Head Neck Surg* 2004;**130**(1):21–7.

34. Garrel R, Dromard M, Costes V, Barbotte E, Comte F, Gardiner Q, et al. The diagnostic accuracy of reverse transcription-PCR quantification of cytokeratin mRNA in the detection of sentinel lymph node invasion in oral and oropharyngeal squamous cell carcinoma: a comparison with immunohistochemistry. *Clin Cancer Res* 2006;**12**(8):2498–505.

35. Seiwert TY, Jagadeeswaran R, Faoro L, Janamanchi V, Nallasura V, El Dinali M, et al. The MET receptor tyrosine kinase is a potential novel therapeutic target for head and neck squamous cell carcinoma. *Cancer Res* 2009;**69**(7):3021–31.

36. Szabo R, Rasmussen AL, Moyer AB, Kosa P, Schafer JM, Molinolo AA, et al. C-Met-induced epithelial carcinogenesis is initiated by the serine protease matriptase. *Oncogene* 2011;**30**(17):2003–16.

37. Cortesina G, Martone T, Galeazzi E, Olivero M, De Stefani A, Bussi M, et al. Staging of head and neck squamous cell carcinoma using the MET oncogene product as marker of tumor cells in lymph node metastases. *Int J Cancer* 2000;**89**(3):286–92.

38. Ferris RL, Xi L, Raja S, Hunt JL, Wang J, Gooding WE, et al. Molecular staging of cervical lymph nodes in squamous cell carcinoma of the head and neck. *Cancer Res* 2005;**65**(6):2147–56.

39. Ferris RL, Xi L, Seethala RR, Chan J, Desai S, Hoch B, et al. Intraoperative qRT-PCR for detection of lymph node metastasis in head and neck cancer. *Clin Cancer Res* 2011;**17**(7):1858–66.

40. Solassol J, Burcia V, Costes V, Lacombe J, Mange A, Barbotte E, et al. Pemphigus vulgaris antigen mRNA quantification for the staging of sentinel lymph nodes in head and neck cancer. *Br J Cancer* 2010;**102**(1):181–7.

41. Wang L, Liu T, Wang Y, Cao L, Nishioka M, Aguirre RL, et al. Altered expression of desmocollin 3, desmoglein 3, and beta-catenin in oral squamous cell carcinoma: correlation with lymph node metastasis and cell proliferation. *Virchows Archiv: Int J Pathol* 2007;**451**(5):959–66.